6 November 1998

Chemical Physics Letters 296 (1998) 421–428

CHEMICAL
PHYSICS
LETTERS

# The bonding of sulfur to Pd surfaces: photoemission and molecular–orbital studies

José A. Rodriguez *, Sanjay Chaturvedi, Tomas Jirsak

*Chemistry Department, Brookhaven National Laboratory, Upton, NY 11973, USA*

Received 6 August 1998

## Abstract

The adsorption and dissociation of $S_2$ on Pd(111) and polycrystalline Pd were studied using synchrotron-based high-resolution photoemission spectroscopy and ab initio SCF calculations. The photoemission results show several sulfur species with distinct electronic properties. The formation of Pd–S bonds induces large positive binding-energy shifts in the core and valence levels of Pd. After chemisorbing sulfur on the Pd surfaces, there is a substantial decrease in the electron density that the metal exhibits near the Fermi level and a simultaneous drop in the electron population of its 4d band. Pd is more sensitive to sulfur than other metals frequently used in automotive exhaust catalysts (Rh and Pt). © 1998 Elsevier Science B.V. All rights reserved.

## 1. Introduction

Palladium is used as a catalysts in several processes in the chemical industry that involve the conversion of hydrocarbons [1]. This metal has high catalytic activity for the selective hydrogenation of olefins, the oxidation of alcohols, and the cyclotrimerization of acetylene [1,2]. Currently, the removal of CO and NO from automobile exhaust ($2CO + O_2 \rightarrow 2CO_2$; $2CO + 2NO \rightarrow 2CO_2 + N_2$) is accomplished by catalytic converters that contain Rh, Pt, or Pd, or a combination of these metals [3,4]. Due to an upgrade in the regulations for the control of environmental pollution, more efficient automotive catalytic converters will be necessary in the future, and it is likely that Pd will be the main component in these devices [5,6]. A major limitation on the useful lifetime of Pd catalysts is sulfur poisoning [1,3,7]. These catalysts are deactivated by sulfur-containing compounds that are present as impurities in all commercial gasolines and petroleum-derived feedstocks. In order to improve the sulfur tolerance of Pd catalysts, one must have a fundamental understanding of how sulfur interacts with Pd surfaces [3,7].

The interaction of $S_2$ with Pd(111) at 300–550 K has been studied using Auger electron spectroscopy (AES), low-energy electron diffraction (LEED), and thermal desorption mass spectroscopy (TDS) [8]. At small doses, the $S_2$ molecule dissociates on the surface, and the results of LEED show $(\sqrt{3} \times \sqrt{3})R30°$ and $(\sqrt{7} \times \sqrt{7})R19.1°$ superstructures. For the $(\sqrt{3} \times \sqrt{3})R30°$ phase, the S atoms occupy fcc hollow sites of the Pd(111) surface [9,10]. At high sulfur cover-

---

* Corresponding author. E-mail: rodrigez@bnl.gov

PII: S0009-2614(98)01011-2

ages ($\theta_S > 0.5$ ML), the formation of a palladium sulfide ($PdS_x$) probably occurs [8].

In this Letter we investigate the adsorption of $S_2$ on Pd(111) and polycrystalline Pd, plus the reaction of Pd atoms with pure sulfur films, using synchrotron-based high-resolution photoemission spectroscopy. The nature of the S–Pd(111) and $S_2$–Pd(111) bonds is examined employing ab initio self-consistent-field (SCF) calculations. The photoemission data show the existence of several sulfur species that have distinct electronic properties. The bonding interactions between S and Pd lead to a large decrease in the density of 4d states that the metal exhibits near the Fermi level. This phenomenon has a strong impact in the chemical and catalytic properties of palladium.

## 2. Experimental and theoretical methods

### 2.1. Synchrotron core-level and valence band data

The photoemission experiments were performed at the U7A end station of the National Synchrotron Light Source (NSLS) at Brookhaven National Laboratory. This beamline is equipped with a toroidal–spherical grating monochromator and an ultrahigh vacuum (UHV) chamber fitted with a hemispherical electron energy analyzer and instrumentation for LEED. The valence and S 2p spectra were acquired using a photon energy of 260 eV, whereas a photon energy of 800 eV was used to take the Pd 3d spectra. The binding energy scale in the photoemission spectra was calibrated by the position of the Fermi edge in the valence region.

Experiments were carried out for the adsorption of $S_2$ on Pd(111) and polycrystalline Pd (thick films of this metal supported on a Rh(111) crystal) at 300 K, and for the reaction of Pd atoms with multilayers (ML) of pure sulfur (also supported on a Rh(111) substrate) at 100 K. The Pd(111) and Rh(111) crystals were cleaned using procedures recommended in previous works [8,11]. $S_2$ was generated inside the UHV chamber by decomposing $Ag_2S$ in a solid-state electrochemical cell: $Pt/Ag/AgI/Ag_2S/Pt$ [11,12]. After applying a voltage across the cell, sulfur evolved predominantly as $S_2$ with a minor 'contamination' of $S_n$ clusters. For small doses of gaseous sulfur, the coverage of sulfur on the sample was determined by measuring the area under the S 2p features, which was scaled to absolute units by comparing to the corresponding area for 0.33 ML of S on Pd(111). Here, we are assuming that the maximum brightness of the ($\sqrt{3} \times \sqrt{3}$)R30° LEED pattern in the S/Pd(111) system corresponds to $\theta_S = 1/3$ [8].

### 2.2. Theoretical calculations

The ab initio SCF calculations described in Section 3 for S/Pd clusters were performed using the HONDO program [13]. The non-empirical effective core potentials of Hay and Wadt were used to describe the inner shells of Pd [14]. The MOs were expanded using Gaussian-type orbitals (GTOs). The atomic orbitals of S were expressed in terms of a double-zeta quality basis set augmented with polarization functions [11,13,15]: 12 s, 8 p, and 1 d primitive GTOs contracted to 6 s, 4 p, and 1 d (12s8p1d/6s4p1d). A basis set obtained through a (3s3p4d/2s1p2d) contraction scheme was used to describe the 5s, 5p and 4d atomic orbitals of Pd [16,17]. Previous experience [11,15,18–20] indicates that this type of ab initio SCF calculations give satisfactory adsorption geometries but underestimate adsorption energies. Due to the approximations in our theoretical approach (size of the basis set, lack of electron correlation, use of finite clusters), the energetics derived from these SCF calculations simply provides a guide for the interpretation of experimental results [11,15,18,19].

## 3. Results and discussion

In previous works [18,21], we have found that thick films of pure sulfur that contain $S_n$ species ($n = 2$–8) can be generated by dosing $S_2$ to metal and oxide substrates at 100 K. These films offer a very convenient route for studying the reaction of metals with sulfur [18,21–23]. Fig. 1 shows S 2p spectra acquired after depositing Pd on a sulfur film (> 15 ML of S supported on a Rh(111) substrate) at 100 K. The deposition of Pd leads to the formation of $PdS_x$ species and new S 2p features appear between 163 and 162 eV. These photoemission features

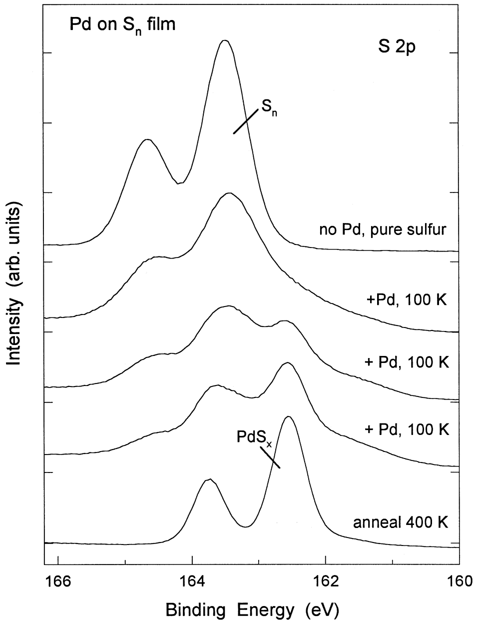

Fig. 1. S 2p spectra acquired after depositing Pd atoms on a thick sulfur film (S$_n$, $n = 2$–8 [21]) at 100 K. In the final step, the sample was annealed to 400 K for 30 s. The spectra were acquired using a photon energy of 260 eV.

become dominant after the third dose of Pd. Annealing to 400 K induces the desorption of the sulfur that is non- or weakly bonded to the metal [21,24], and one is left with a film of PdS$_x$. At this point the S 2p spectrum shows a very well-defined doublet, which indicates that only one type of sulfur species is present in the system. The S 2p$_{3/2}$ peak appears at an energy (∼ 162.5 eV) that is typical of S atoms bonded to metals [11,20,23] (i.e. no significant S ↔ S interactions in the system).

The top panel in Fig. 2 displays the corresponding valence spectra for the experiments in Fig. 1. In the valence spectrum for pure sulfur, the S 3p levels give rise to a peak at ∼ 3 eV and a broad feature from 5 to 9 eV [21]. Upon dosing of Pd at 100 K, new features appear from 2 to 0 eV as a consequence of electron emissions from the occupied Pd 4d orbitals. After annealing to 400 K, the formed PdS$_x$ exhibits two main features: one between 8 and 4 eV in which the S 3p contributions are important, and one from 4 to 0 eV dominated by the Pd 4d band. If one compares this spectrum with that of metallic Pd (for example, see valence spectrum for clean Pd(111) in bottom panel of Fig. 2), one finds that the sulfide has a very small density of states in the region near the Fermi level (0 of binding energy). The Pd ↔ S interactions shift the Pd 4d valence band toward higher binding energy. An identical trend was observed for the Pd 3d core levels (see top panel in Fig. 3). The Pd atoms embedded in the sulfur film displayed Pd 3d$_{5/2}$ binding energies that were 1.5–1.9 eV larger than that reported for bulk Pd (335.2 eV [25], vertical line in top panel of Fig. 3). These binding-energy shifts are within the range of values seen for the binding-energy shifts of compounds in which Pd has a formal oxidation state of $+2$ (1–1.5 eV) or $+4$ (1.5–2.5 eV) [26].

The photoemission data for the Pd/S and PdS$_x$ systems indicate that sulfur can induce large changes

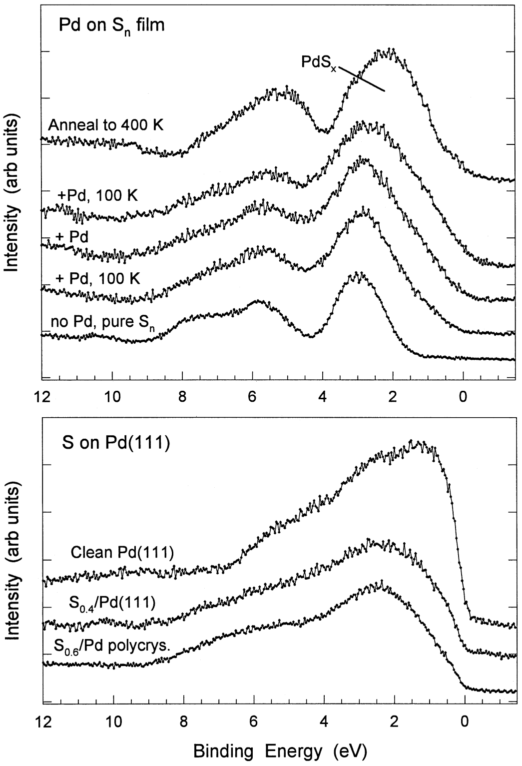

Fig. 2. Top panel: valence band spectra for the deposition of Pd on a pure sulfur film (> 15 ML) at 100 K. In the final step, the sample was annealed to 400 K. Bottom panel: valence spectra for clean Pd(111), a Pd(111) surface with 0.4 ML of sulfur, and a polycrystalline surface of Pd with 0.6 ML of S. All the spectra were taken using a photon energy of 260 eV.

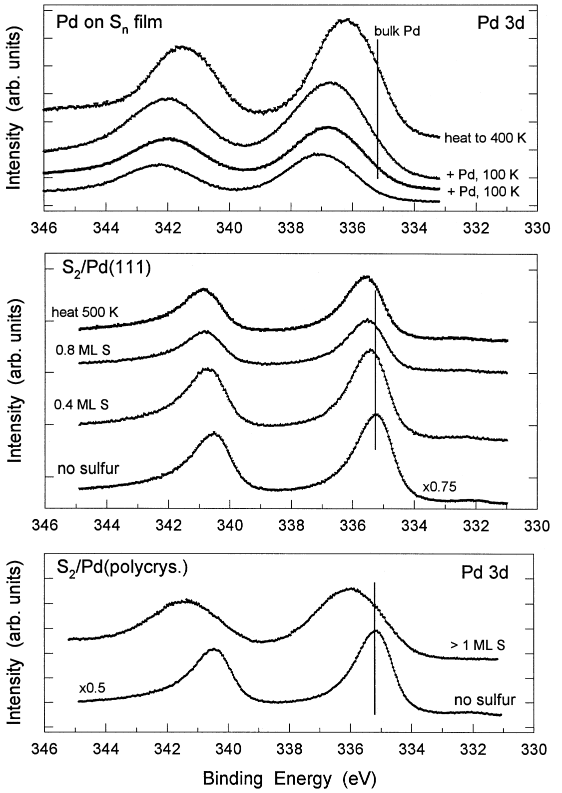

Fig. 3. Top: Pd 3d spectra for the deposition of Pd atoms on a pure sulfur film at 100 K. In the final step, the sample was heated to 400 K for 30 s. The vertical line denotes the position reported [25] for the Pd $3d_{5/2}$ level of bulk Pd (335.2 eV). Middle: Pd 3d spectra for clean Pd(111), $S_{0.4}$/Pd(111) and $S_{0.8}$/Pd(111) surfaces at 300 K, and a $S_{0.8}$/Pd(111) surface heated to 500 K. The vertical line indicates the center of the Pd $3d_{5/2}$ peak of clean Pd(111). Bottom: Pd 3d spectra for polycrystalline palladium before and after dosing $S_2$ at 300 K. The vertical line denotes the center of the Pd $3d_{5/2}$ peak of the clean polycrystalline surface. All the spectra were acquired using a photon energy of 800 eV.

in the electronic properties of Pd. Substantial electronic perturbations are also found after chemisorbing sulfur on Pd(111) or polycrystalline Pd. The bottom panel in Fig. 2 shows valence spectra for Pd surfaces partially covered with sulfur: 0.4 ML of S on Pd(111), and 0.6 ML of S on polycrystalline Pd. In these systems, it is not easy to isolate the valence photoemission features that are only due to S-bonded Pd atoms. But, since at a photon energy of 260 eV the S 3p signal from sub-monolayer coverages of sulfur is not expected to dominate the valence spectra [11], it is clear that the chemisorption of S leads to a reduction in the density of Pd 4d states near the Fermi level. For clean Pd(111), the 4d band exhibits a maximum at ~ 1.2 eV. At this binding energy, the $S_{0.4}$/Pd(111) system shows relatively weak emissions and its valence-band maximum appears at ~ 2.5 eV. These differences reflect the trends seen when comparing the valence spectra of metallic Pd and $PdS_x$. Previous studies for S/Rh(111) [11], S/Rh(100) [27], S/Pt(111) [20] and S/W(100) [28] show a S-induced decrease in the density of states that the metal substrates display around the Fermi level.

In Fig. 3, we can see Pd 3d spectra for clean and sulfur covered Pd(111). In these photoemission experiments there was not enough resolution to separate contributions from the bulk and surface atoms of the Pd(111) system. After depositing 0.4 and 0.8 ML of S on Pd(111) at 300 K, one sees Pd $3d_{5/2}$ binding-energy shifts of ~ 0.3 and 0.5 eV (respectively). Upon annealing of $S_{0.8}$/Pd(111) to 500 K, part of the sulfur migrates into the subsurface region [8] and there is a slight increase in the intensity of the Pd 3d signal plus an additional binding-energy shift of ~ 0.15 eV. Polycrystalline Pd was much more reactive towards $S_2$ than Pd(111). On the polycrystalline surface, it was very easy to form films of $PdS_x$ and large changes were observed in the Pd 3d region. A typical result is shown in the bottom panel of Fig. 3. The reaction with $S_2$ induces a broadening of the Pd 3d features with a positive shift of ~ 1 eV in their peak positions.

Fig. 4 displays photoelectron spectra from the S 2p core levels of several S/Pd(111) and S/Pd (polycrystalline) surfaces. At sulfur coverages below 0.4 ML, only a single doublet of peaks is observed in the S 2p region and can be assigned to atomic S [21,24]. For large sulfur coverages, the complex line shape of the S 2p features indicates that more than one type of S species is present on the surface. The spectral weight above 163 eV can be attributed to species in which there are significant S ↔ S bonding interactions [21,24]. For the S/Pd(111) system, the results of LEED [8,9] and STM [10] show a $(\sqrt{3} \times \sqrt{3})R30°$ structure at $\theta_S \leqslant 0.33$ ML with the S atoms sitting on fcc hollow sites of the surface [9]. This sulfur species is responsible for the well-defined S 2p doublets seen in Fig. 4 for S/Pd(111) at $\theta_S \leqslant 0.33$ ML. When the S coverage rises above 0.4 ML, there

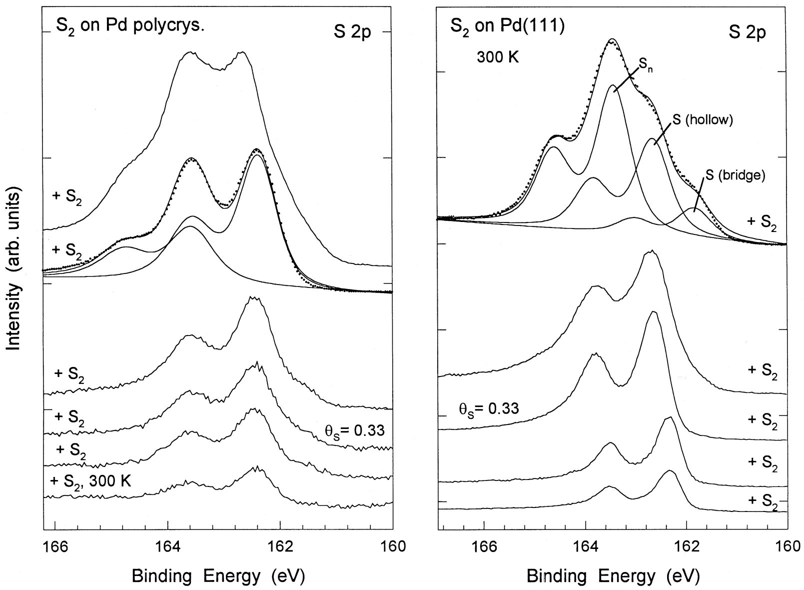

Fig. 4. S 2p spectra for the adsorption of $S_2$ on Pd(111) (right panel) and polycrystalline Pd (left panel). Sulfur was dosed at 300 K. The spectra at the top of the figure were curve-fitted following the procedure described in Refs. [20] and [21]. In these cases, the raw data are plotted as dots. The spectra were taken using a photon energy of 260 eV.

is a rapid decline of the LEED spots and the adlayer becomes disordered on the Pd(111) surface [8]. Following this pathway the S 2p spectra of the S/Pd(111) system show substantial changes, First, the single doublet becomes ill defined, and then new features appear toward higher binding energy. At this point, the complex S 2p spectrum is well fitted with a set of three doublets that can be assigned [11,20] to adsorbed $S_n$ species plus atomic S on hollow and bridge sites of the surface (see Fig. 4). In general, a difference of ~ 1 eV is found when comparing the S $2p_{3/2}$ binding energies of sulfur atoms adsorbed on hollow and bridge sites of W(100) [28], Pt(111) [20] and Rh(111) [11]. As we will see below, this difference reflects variations in the electron density of the S adatoms (hollow < bridge).

The bonding interactions between Pd(111) and S or $S_2$ were examined using ab initio SCF calculations. Fig. 5 shows the 12-atom cluster used to model the metal surface. A S atom was set above one of the following adsorption sites: the center of the fcc hollow site formed by the atoms labeled A and B (ABB), the middle of the bridge site between the A atom and one of the B atoms (AB), or a-top atom A (A). In all the cases studied, the Pd–Pd separations were set equal to 2.75 Å as in bulk Pd. The S–Pd nearest neighbor distances were optimized at the ab initio SCF level and the calculated values are listed in Table 1. The predicted value for S on the hollow site (2.26 Å) is close to the values obtained in LEED studies (2.22–2.25 Å) for the $(\sqrt{3} \times \sqrt{3})R30° - S/Pd(111)$ superstructure [9]. On the hollow ABB site the adsorption energy of S was 7 and 12 kcal/mol larger than on the bridge AB and a-top A sites, respectively. Therefore, at low coverages, S should sit on hollow sites of the surface. Table 1 shows calculated charges [1] and atomic orbital populations for different conformations of the $S/Pd_{12}$ cluster. In general, S behaves as a weak electron acceptor when bonded to Pd(111). The negative charge on the adatom is mainly a consequence

---

[1] The charges were calculated using a Mulliken population analysis [29]. Due to the limitations of this type of analysis [29], the charges must be interpreted only in qualitative terms. They provide a ‘rough’ idea of the degree of ionicity in the Pd–S and Pd–$S_2$ bonds.

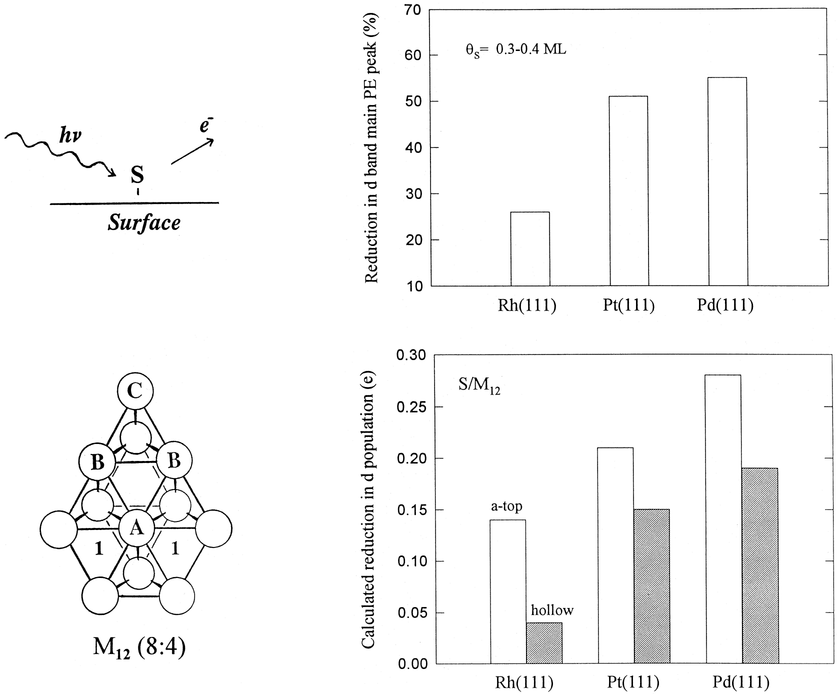

Fig. 5. Left side bottom: metal cluster, $M_{12}$, used to model the adsorption of sulfur on Rh(111), Pt(111), and Pd(111). Right side bottom: results of ab initio SCF calculations for $S/Rh_{12}$ [11], $S/Pt_{12}$ [20] and $S/Pd_{12}$ (Table 1) clusters. The graph shows the reduction in the valence d population of the A atom in the $M_{12}$ cluster upon the adsorption of S above A (a-top, empty bars) and on the hollow ABB site (hatched bars). Right side top: results of photoemission (PE) measurements for $S_{0.4}$/Rh(111) [11], $S_{0.3}$/Pt(111) [20] and $S_{0.4}$/Pd(111) (Fig. 2). The graph displays the percentage decrease induced by sulfur on the intensity of the main peak (located at 0–1 eV below the Fermi level) in the Rh 4d, Pt 5d and Pd 4d bands.

of a Pd(4d,5s) → S(3p) electron transfer. On the hollow ABB site, the charge is smaller than on the bridge AB or a-top A site. For hollow adsorption, the S adatoms are forced to make bonds through their occupied 3s and 3p orbitals. This leads to a more covalent adsorption bond, in which part of the charge that is transferred from the surface into the vacant S(3p) orbitals is compensated by charge transfer from the occupied S(3s,3p) orbitals into the empty bands of the Pd substrate. The formation of Pd–S bonds induces a large decrease in the electron population of the Pd 4d states, see Table 1, as a result of a Pd(4d) → S(3p) electron transfer and a Pd(4d) → Pd(5s,5p) orbital rehybridization. From previous theoretical [16,17,30,31] and experimental [32,33] works, it is known that Pd has a big tendency to 'lose' 4d electrons and 'gain' 5s,p electrons when forming chemical bonds. The drop in the Pd 4d population seen in the model cluster is important and correlates well with the trends observed in the photoemission experiments for the $PdS_x$ and S/Pd systems.

In Table 2 are listed calculated structural parameters and adsorption energies for $S_2$ on a-top and

Table 1
$S/Pd_{12}$ cluster: atomic orbital populations and charges (electrons)[a]

| S on | Pd–S bond (Å) | Pd (A)[b] populations 4d | 5s,p | charge | Sulfur charge |
|---|---|---|---|---|---|
| hollow (ABB) | 2.26 | 9.55 | 0.30 | 0.15 | −0.24 |
| bridge (AB) | 2.24 | 9.42 | 0.28 | 0.23 | −0.35 |
| a-top (A) | 2.21 | 9.46 | 0.22 | 0.31 | −0.38 |
| no sulfur | – | 9.74 | 0.19 | 0.07 | – |

[a] From a Mulliken population analysis.
[b] The values listed are for the Pd atom labeled 'A' in Fig. 5.

Table 2
Adsorption of $S_2$ on $Pd_{12}$

| | Pd–S bond (Å) | S–S bond (Å) | Charge on $S_2^a$ (e) | Adsorption energy [b] (kcal/mol) |
|---|---|---|---|---|
| Free $S_2$ | – | 1.88 | – | – |
| On Pd(111) | | | | |
| Vertical (A) | 2.29 | 1.97 | −0.09 | 16 |
| Parallel (A) | 2.37 | 2.02 | −0.17 | 20 |
| Bridge (BB) | 2.34 | 2.07 | −0.22 | 24 |
| Bridge (AC) | 2.36 | 2.12 | −0.23 | 27 |
| 2 S atoms (1,1) | 2.28 | – | −0.44[c] | 52 |

[a] From a Mulliken population analysis.
[b] A positive value denotes an exothermic adsorption process. The adsorption energy was calculated using the $S_2$ molecule and the isolated $Pd_{12}$ cluster as reference state.
[c] Sum of the charge on the two sulfur atoms.

bridge sites of the $Pd_{12}$ cluster. The molecule was adsorbed on top of the $Pd_A$ atom with its molecular axis either vertical (one Pd–S bond) or parallel (two equivalent Pd–S bonds) to the surface. In addition, we also studied bridging configurations (Pd–S–S–Pd) in which the molecule was bonded to the two $Pd_B$ atoms, or to the $Pd_A$ and $Pd_C$ atoms. On the $Pd_{12}$ cluster, the $S_2$ molecule is more stable when both S atoms are simultaneously bonded to the metal substrate. The ground $^3\Sigma_g^-$ state of $S_2$ arises from a $4\sigma_g^2 4\sigma_u^2 5\sigma_g^2 2\pi_u^4 2\pi_g^2$ electronic configuration. The $2\pi_g$ orbitals are only half occupied. The bonding mechanism of $S_2$ to Pd(111) involves a donation of charge from the S–S bonding $2\pi_u$ and $5\sigma_g$ orbitals into the surface, and back donation of electrons from the surface into the S–S antibonding $2\pi_g$ orbitals. The combination of these two phenomena leads to a substantial weakening and elongation of the S–S bond (0.09–0.24 Å). The larger the charge transfer from Pd into the $S_2(2\pi_g)$ orbital, the bigger the adsorption energy of the molecule and the elongation of the S–S bond. Bonding configurations in which $S_2$ bridges two palladium atoms ($Pd_B$–S–S–$Pd_B$ and $Pd_A$–S–S–$Pd_C$) are probable precursors for the dissociation of the molecule. In the SCF calculations, we found that two separate sulfur adatoms are much more stable on the $Pd_{12}$ cluster than $S_2$ bonded in any configuration. Therefore, molecular adsorption of $S_2$ on Pd(111) can occur only at the limit of high coverages when there are not enough empty sites for a dissociation process.

The modifications induced by sulfur on the Pd 4d band can lead to significant changes in the chemical and catalytic properties of the metal. In general, one can expect a decrease in the activity of Pd for adsorption reactions that involve donation of electrons to the adsorbate ($H_2$, CO, NO, olefins, etc.). For example, sulfur should hinder the dissociation of $H_2$ on Pd surfaces [34,35]. It is worthwhile to examine in detail how sulfur affects the bands of the three metals most frequently used in automotive exhaust catalysts (Rh, Pt and Pd) [3,4]. The top panel in the right side of Fig. 5 compares the decrease induced by S on the intensity of the metal d features that appear 0–1 eV immediately below the Fermi level in $S_{0.4}$/Rh(111) [11], $S_{0.3}$/Pt(111) [20] and $S_{0.4}$/Pd(111). In a $S_{0.4}$/Rh(111) surface, sulfur produces a reduction of ~25% in the density of states near the Fermi level [11], whereas in $S_{0.4}$/Pd(111) the corresponding reduction is close to 55% (Fig. 2). The results of ab initio SCF calculations indicate that S also produces decreases in the valence d population of the metals. The bottom panel in the right side of Fig. 5 compares the d-population reduction calculated for an A atom in $S/Rh_{12}$ [11], $S/Pt_{12}$ [20] and $S/Pd_{12}$ (Table 1) when sulfur is adsorbed above the A atom or on the hollow ABB site. In the $S/M_{12}$ clusters, the tendency of a metal to lose d electrons increases in the following order: $Rh < Pt < Pd$. This agrees well with the relative occupancy of the d shell in the isolated elements: Rh, $d^8s^1$ < Pt, $d^9s^1$ < Pd, $d^{10}s^0$. By comparing the trends in Fig. 5, a clear correlation is seen between the change in the d population of a metal and the attenuation in its density of states near the Fermi level. *Pd shows the biggest drop in the d population and the largest attenuation in the density of states*. The electronic perturbations in Fig. 5 indicate that Pd should be more affected by sulfur than Rh. Indeed, automotive exhaust catalysts based on Pd are more sensitive to sulfur poisoning than catalysts based on Rh [3].

## 4. Conclusions

The formation of Pd–S bonds induces large positive binding-energy shifts in the core and valence levels of palladium. After chemisorbing sulfur on Pd(111) or polycrystalline Pd, there is a substantial decrease in the density of states that the metal exhibits near the Fermi level and a simultaneous drop in the electron population of the Pd 4d band. On Pd(111) at 300 K, S is bonded to two dissimilar adsorption sites (hollow and probably bridge) that show well-separated S 2p binding energies and different bonding interactions. At sulfur coverages above 0.5 ML, $S_n$ species appear on the surface and are the precursors for the generation of palladium sulfides.

## Acknowledgements

This work was supported by the US Department of Energy, Office of Basic Energy Sciences, Chemical Science Division (DE-AC02-98CH10886). TJ acknowledges the support of NATO under a Grant awarded in 1997.

## References

[1] G. Ertl, H. Knözinger, J. Weitkamp (Eds.), Handbook of Heterogeneous Catalysis, Wiley–VHC, Weinheim, 1997.
[2] R.M. Lambert, R.M. Omerod, in: R.J. Madix (Ed.), Surface Reactions, vol. 34, Springer Series in Surface Science, chap. 4, Springer, Berlin, 1994.
[3] K.C. Taylor, Catal. Rev. Sci. Eng. 35 (1993) 457.
[4] M. Shelef, G.W. Graham, Catal. Rev. Sci. Eng. 36 (1994) 433.
[5] R.W. McCabe, R.K. Usmen, Studies Surf. Sci. Catal. 101 (1996) 355.
[6] D.D. Beck, J.W. Sommers, C.L. DiMaggio, Appl. Catal. B 3 (1994) 205.
[7] C.H. Bartholomew, P.K. Agrawal, J.R. Katzer, Advan. Catal. 31 (1982) 135.
[8] C.H. Patterson, R.M. Lambert, Surf. Sci. 187 (1987) 339.
[9] M.E. Grillo, C. Stampfl, W. Berndt, Surf. Sci. 317 (1994) 84.
[10] J.G. Forbes, A.J. Gellman, J.C. Dunphy, M. Salmeron, Surf. Sci. 279 (1992) 68.
[11] J.A. Rodriguez, S. Chaturvedi, M. Kuhn, J. Chem. Phys. 108 (1998) 3064.
[12] W. Heegemann, K.H. Meister, E. Bechtold, K. Hayek, Surf. Sci. 49 (1975) 161.
[13] M. Dupuis, S. Chin, A. Marquez, in: G.L. Malli (Ed.), Relativistic and Electron Correlation Effects in Molecules and Clusters, NATO ASI Series, Plenum Press, New York, 1992.
[14] P.J. Hay, W.R. Wadt, J. Chem. Phys. 82 (1985) 270.
[15] S. Chaturvedi, J.A. Rodriguez, J. Hrbek, J. Phys. Chem. B 101 (1997) 10860.
[16] J.A. Rodriguez, Surf. Sci. 345 (1996) 347.
[17] J.A. Rodriguez, M. Kuhn, J. Phys. Chem. 100 (1996) 381.
[18] J.A. Rodriguez, T. Jirsak, S. Chaturvedi, J. Hrbek, Surf. Sci. 407 (1998) 171.
[19] J.A. Rodriguez, S. Chaturvedi, M. Kuhn, J. Hrbek, J. Phys. Chem. B 102 (1998) 5511.
[20] J.A. Rodriguez, M. Kuhn, J. Hrbek, Chem. Phys. Lett. 251 (1996) 13.
[21] J. Hrbek, S.Y. Li, J.A. Rodriguez, D.G. van Campen, H.H. Huang, G.-Q. Xu, Chem. Phys. Lett. 267 (1997) 65.
[22] J.A. Rodriguez, Polyhedron 16 (1997) 3177.
[23] J.A. Rodriguez, S.Y. Li, J. Hrbek, H.H. Huang, G.-Q. Xu, Surf. Sci. 370 (1997) 85.
[24] S.Y. Li, J.A. Rodriguez, J. Hrbek, H.H. Huang, G.-Q. Xu, Surf. Sci. 366 (1996) 29.
[25] G.P. Williams, Electron Binding Energies of the Elements, National Synchrotron Light Source, Brookhaven National Laboratory, version II, January 1992.
[26] C.D. Wagner, W.M. Riggs, L.E. Davis, J.F. Moulder, G.E. Muilenberg, Handbook of X-Ray Photoelectron Spectroscopy, Perkin–Elmer, Eden Pririe, MN, 1978, p. 110.
[27] P.J. Feibelman, Phys. Rev. B 41 (1990) 11881.
[28] D.R. Mullins, P.F. Lyman, S.H. Overbury, Surf. Sci. 277 (1992) 64, and references therein.
[29] A. Szabo, N.S. Otslund, Modern Quantum Chemistry, McGraw–Hill, New York, 1989.
[30] G. Pacchioni, R.M. Lambert, Surf. Sci. 304 (1994) 208.
[31] A. Rochefort, R. Fournier, J. Phys. Chem. 100 (1996) 13506.
[32] Y. Yeon, J. Chen, M. Croft, Phys. Rev. B 50 (1994) 6555.
[33] T.K. Sham, Phys. Rev. B 31 (1985) 1903.
[34] M.L. Burke, R.J. Madix, Surf. Sci. 237 (1990) 1.
[35] S. Wilke, M. Scheffler, Phys. Rev. Lett. 76 (1996) 3380.